AN OVERVIEW OF PROGRESS WITH THE STUDY OF A STRUCTURED LASER BEAM FOR ALIGNMENT

Witold NIEWIEM[1,2], Dirk MERGELKUHL[1], Jean-Christophe GAYDE[1]

[1] CERN, Geneva, Switzerland
[2] ETH, Zurich, Switzerland

Abstract

The Structured Laser Beam (SLB) is a pseudo-non-diffractive optical beam characterized by the low divergence of the Inner Core (IC), down to 10 µrad, and the presence of concentric rings, with the most prominent being the Outer Ring (OR). The size of the IC and OR can vary depending on the SLB generator setup. SLBs have the potential to serve as straight reference lines for long-distance alignment systems due to the small diameter of their IC and theoretically infinite propagation distance, which has been experimentally verified up to 900 m. However, the straightness of a light beam propagating in the atmosphere can be affected by refraction. Optical alignment systems often use a vacuum to mitigate this refraction effect. While creating such a vacuum system provides a propagation space for the laser beam, it imposes constraints on space availability, access, and the operation of the alignment system. In the case of an SLB passing through a vacuum pipe, the intensity distribution may be modified, resulting in an apparent shift of the IC and disrupting the straight reference line. Additionally, light reflected from the vacuum pipe complicates the measurement of the IC position. This paper discusses the prospects of SLB alignment systems, including recent advancements and remaining challenges.

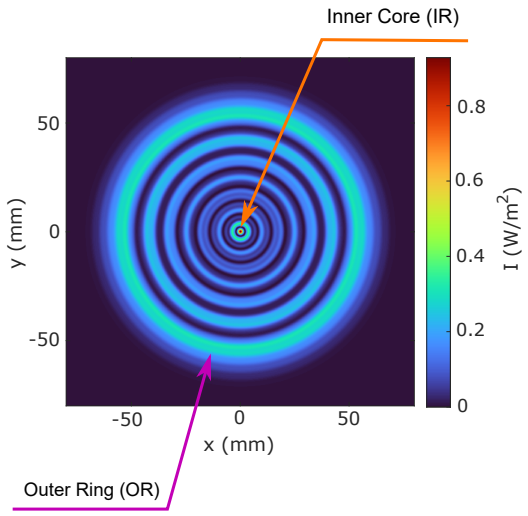

Figure 1: The simulated transversal intensity distribution of an SLB at 225 m from the generator with the IC and OR indicated.

INTRODUCTION

A Structured Laser Beam (SLB) is a pseudo-non-diffractive optical beam that can be placed within the broader category of structured light. The transversal intensity profile of an SLB features a narrow Inner Core (IC) surrounded by concentric rings, with the Outer Ring (OR) being the most prominent [1, 2], as presented in Fig. 1. The SLB profile is similar to that of a Bessel beam, previously used for alignment purposes [3–5]. Due to the low divergence of the IC, down to 10 µrad, and its theoretically infinite propagation distance, SLBs are promising for establishing a straight reference line for long-distance alignment. This propagation distance has been experimentally tested up to 900 m, a task unfeasible with Bessel beams due to their finite propagation distance [6].

Large particle accelerators can span kilometers in circumference and are subject to stringent geometrical requirements demanding precise alignment within tens of microns across distances of some hundreds of meters [7]. Conventional methods for measuring particle accelerators typically involve leveling and polar measurements [8]. However, alternative methods, such as measurement with respect to the straight reference line and hydrostatic leveling, are employed to meet the most demanding accuracy requirements of the largest accelerators [9].

The measurement with respect to the straight reference line can be established using either a physical or an optical line. The distance between an object and the reference line is measured with respect to this reference line. Measurements based on an optical line typically use a laser beam. A significant challenge in long-distance laser beam propagation is light divergence. The divergence makes detecting the laser spot more difficult as the distance gets larger and the spot size increases, so larger detectors are required. Various methods have been proposed in the past to address this issue [10–12]. Due to its low IC divergence, the SLB is a strong candidate for replacing the classical Gaussian beam characterized by relatively large divergence [13].

Atmospheric variations causing changes in the local refractive index bends laser beams, precluding high-precision alignment. To mitigate this, SLAC introduced a vacuum pipe with a pressure of around 0.01 mbar [10]. Following SLAC's lead, vacuum systems were also adopted at KEK [14] and DESY [11]. While low pressure effectively reduces the refraction impact, it introduces challenges related to the pumping process and the mechanical connection between

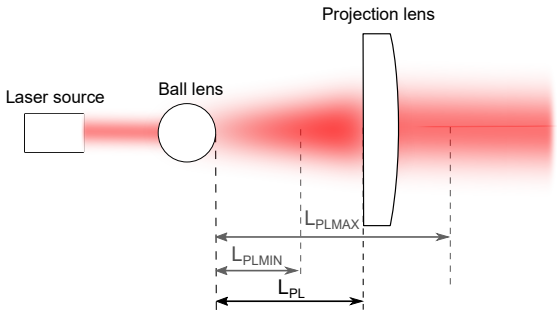

Figure 2: Schematic of the SLB generator with the laser source, the ball lens, the projection lens, and distances L_{PL}, L_{PLmax}, L_{PLmin}.

the vacuum-enclosed sensor and the measured component. It also poses issues for SLBs.

Simulations and experiments have characterized the divergence of the IC and OR [2]. Symmetry breaking occurs when the SLB's light path is altered by passing through an aperture that partially obstructs the transversal profile area [15]. This alteration can negatively impact alignment applications. Reflections from the pipe surface reach the sensor, overlaying the direct SLB pattern and causing interference. The resulting noise degrades the beam's geometry and can lead to disturbances of the straight reference line. In astronomy, black coatings are commonly used to reduce reflection noise [16]. Another effective approach is the use of baffles [17]. Combining these two methods provides a reliable reduction of noise induced by reflections.

This paper provides an overview of the SLB project, summarizing aspects of the SLB generation, the IC and OR divergence, IC detection, vacuum systems, symmetry breaking, and reflections in the vacuum pipe.

GENERATION AND WAVEFRONT

An SLB can be generated using multiple generator layouts [1]. The generator used in the investigation consists of a laser source, a ball lens, and a plano-convex projection lens, as illustrated in Fig. 2. Modifying these elements or their mutual positions affects the SLB wavefront and intensity distribution. The distance between the ball lens and the projection lens L_{PL} impacts the transversal intensity profile of an SLB and defines the generator's focus.

To facilitate comparison between different generators, L_{PL} is replaced by the parameter ξ [2]. The ξ parameter describes the relative position of the chosen value of L_{PL} between two extreme values L_{PLmin} and L_{PLmax}, see Eq. 1. For $\xi > 1$, SLBs are formed within a constrained range, beyond which the IC and OR vanish, akin to the behavior of Bessel beams. When $\xi < 0$, SLBs do not form, and the IC does not appear.

$$L_{PL} = L_{PLmin} + \xi(L_{PLmax} - L_{PLmin}) \tag{1}$$

The SLB wavefront h_s combines two rotationally symmetric optical effects with opposite signs: spherical aberration

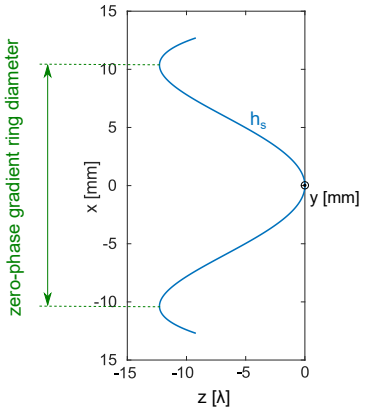

Figure 3: The cross-section of the SLB wavefront h_s with zero-phase gradient ring.

and defocus. The wavefront is characterized by a zero-phase gradient ring as visible in Fig. 3.

The generator parameters influence the wavefront, which in turn affects the transversal intensity profile at a given position. Increasing the size of the projection lens results in a larger diameter of the zero-phase gradient ring, which subsequently reduces the IC. Conversely, a longer focal length of the projection lens results in a smaller OR, thereby optimizing the generator's performance for long-distance alignment purposes.

INTENSITY PROFILE

Fig. 4 presents the size of the IC and OR depending on the focusing of the generator expressed by ξ at a given distance. The blue lines show the numerical simulations for propagation distances of 30 m, 40 m, and 50 m. The lines correspond to different values of ξ, ranging from $\xi = 0$ to $\xi = 1$.

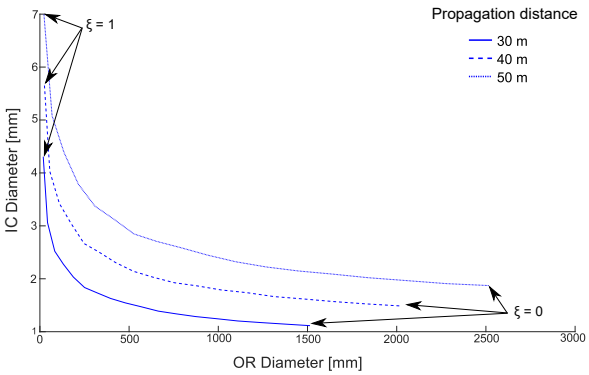

Figure 4: Simulation of the IC and OR size for different distances and generator focus.

The trade-off between the size of the IC and OR is crucial for the alignment system's performance. On the one hand, the IC defines the minimal size of the sensor that is required at a given position. On the other hand, the OR should not

violate the propagation space of the system established by the alignment vacuum tube, as this may be detrimental due to symmetry breaking of the SLB and reflections.

In Fig. 5, the simulation of the OR diameter as a function of propagation distance is presented. In the near optical zone, the dependence is not linear, but beyond this, at distances > 9 m for this specific generator layout, the OR increases proportionally to the propagation distance [2].

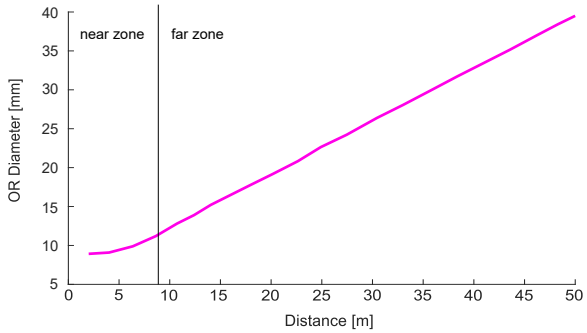

Figure 5: The simulation of the OR size for different propagation distances.

The SLB propagation can be described using two longitudinal zones. The boundary between the near and far optical zones is defined by the behavior of the transversal intensity. In the near zone, the pattern and divergence of an SLB vary with the longitudinal position. In contrast, in the far zone, the pattern scales linearly and the divergence remains constant. It is important to note that in the near zone, the divergence of the IC and OR is non-linear. For long-distance alignment applications, propagation typically occurs in the far zone, where SLB divergence is approximately linear with distance.

IC POSITION DETECTION

The position of the IC is measured to determine the optical axis of the SLB, which in turn defines the straight reference line. In previous research on SLBs, the IC was detected using three algorithms: Bessel beam fitting, center of gravity, and correlation with a 2D Gaussian beam.

The Bessel beam fitting method is based on the similarity between the center of a Bessel beam and an SLB. The parameters of the Bessel function, as shown in Eq. 2, are optimized to achieve maximal agreement between the theoretical Bessel function and the simulated or measured SLB.

$$I(x,y) = \left(J_0\left(k_T\sqrt{(x-x_0)^2+(y-y_0)^2}\right)\right)^2 \tag{2}$$

$I(x,y)$ is intensity, J_0 represents the Bessel function of the first kind and zero order, k_T is the transverse wave vector, and x_0, y_0 are the coordinates of the Bessel beam center [2].

The other method of calculating the IC position is the weighted center of gravity algorithm. It computes the centroid of the IC $(\bar{x}, \bar{y})$ following Eq. 3 and Eq. 4.

$$\bar{x} = \frac{\sum_{x=0}^{x_{\max}}\sum_{y=0}^{y_{\max}} I(x,y)\cdot x}{\sum_{x=0}^{x_{\max}}\sum_{y=0}^{y_{\max}} I(x,y)} \tag{3}$$

$$\bar{y} = \frac{\sum_{x=0}^{x_{\max}}\sum_{y=0}^{y_{\max}} I(x,y)\cdot y}{\sum_{x=0}^{x_{\max}}\sum_{y=0}^{y_{\max}} I(x,y)} \tag{4}$$

In the preprocessing step, pixel intensities are adjusted either through the gamma function or by thresholding to exploit the existing differences between the intensities of the IC and the rings, thereby separating the two features. Additionally, the algorithm is employed twice: first, to define the approximate region of interest and crop the image to the IC, and second, to determine the final position of the IC center [18].

The third algorithm developed for IC position detection is correlation template matching. The correlation function $C(\bar{x}, \bar{y})$, as shown in Eq. 5, is used to compare the 2D Gaussian template $t(x,y)$ with the measured transversal intensity profile.

$$C(\bar{x},\bar{y}) = \frac{\sum_{x,y}\left|I(x,y)-\overline{I_{u,v}}\right|\left[t(x-\bar{x},y-\bar{y})-\bar{t}\right]}{\left\{\sum_{x,y}\left|I(x,y)-\overline{I_{u,v}}\right|^2\sum_{x,y}\left[t(x-\bar{x},y-\bar{y})-\bar{t}\right]^2\right\}^{0.5}} \tag{5}$$

$\bar{t}$ is the average intensity of the template function, and $\overline{I_{u,v}}$ is the average intensity of the transversal intensity profile in the feature region. The algorithm is adjusted to the specific transversal profile of an SLB. The size of the template and its standard deviation are set up based on average IC size and intensity [18].

The proposed algorithms perform well on simulated SLBs. However, their robustness to the noise present in the empirical data can vary. The most numerically efficient method is a weighted center of gravity algorithm.

VACUUM SYSTEM

Vacuum systems mitigate refraction in a non-homogeneous medium. Although effective, such systems may encounter issues due to the contraction of the vacuum chamber, which can affect alignment accuracy. As the vacuum system reaches operational pressure, it can shrink, potentially disrupting the relative position between the sensor and the measured object. The deformation of a 70 m vacuum system with a single fixed point at one end is shown in Fig. 4. The majority of the deformation occurs at the start of pumping, with less deformation once reaching 1 mbar.

Vacuum systems meet stringent requirements for tightness and cleanliness, making them both costly and delicate components of the alignment setup. Vacuum pipes are usually designed with a limited diameter to minimize costs and conserve space in valuable underground environments. This constraint can lead to symmetry breaking, which can cause deviations in the straight reference line of the SLB. Additionally, the propagation of an SLB through a stainless steel

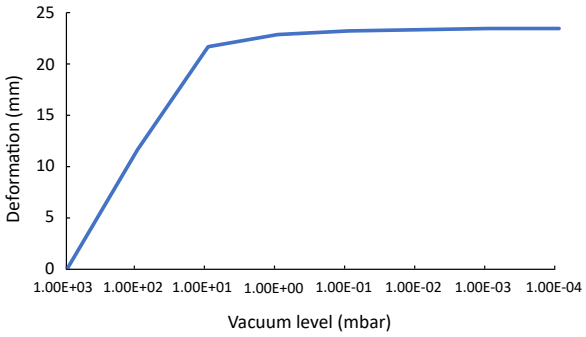

Figure 6: The shrinkage of a 70 m vacuum system depending on the pressure in the system.

vacuum pipe may result in light reflections, which can degrade the quality of the detected image due to interference from both direct and reflected light reaching the sensor.

SYMMETRY BREAKING

Symmetry breaking occurs when an SLB passes through an obstacle that covers part of its transversal intensity profile. In accelerator alignment, a common obstacle in the propagation path is the vacuum pipe used to avoid atmospheric turbulence, which creates a continuous aperture. When the symmetry of the SLB profile is disrupted, the IC that defines the straight reference line is disturbed, potentially corrupting the reference line. The IC geometry and detected position can depend on the generator parameters, the longitudinal and transversal position of the obstacle, and the longitudinal position of the target plane where the SLB profile is detected.

Fig. 7 presents the simulated effect of SLB symmetry breaking. The distance between the generator and the target plane where the light detector is placed is 140 m. The SLB generator layout is configured such that the OR at 70 m has approximately the same diameter as the aperture. A circular aperture of 50 mm diameter is introduced at 70 m. With the center of the aperture at position $x = 0$ mm, the aperture is perfectly centered around the SLB and does not interact with the outer ring. The edge of the aperture passes through the middle of the theoretical IC position when the aperture is misaligned by 25 mm.

The calculated IC position shift reaches a maximum of ±0.3 mm. A trade-off between the generator setup and the diameter of the vacuum system therefore has to be found to avoid affecting the straight reference line.

REFLECTION NOISE

A 156 mm diameter vacuum pipe system, made of stainless steel, creates the low-pressure area along the entire SLB propagation path. However, the high reflectivity of the interior walls diminishes the signal-to-noise ratio of the detected IC and lowers the accuracy of IC position measurement. This stray light contributes to significant noise due to interference with the direct SLB pattern Fig. 8.

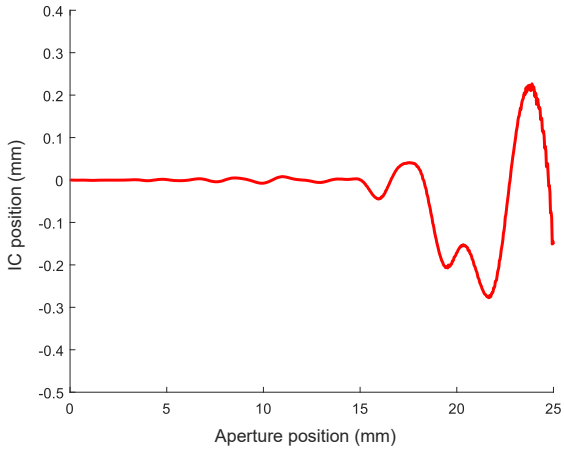

Figure 7: The simulated IC position at 140 m depending on the misalignment of a 50 mm circular aperture at 70 m.

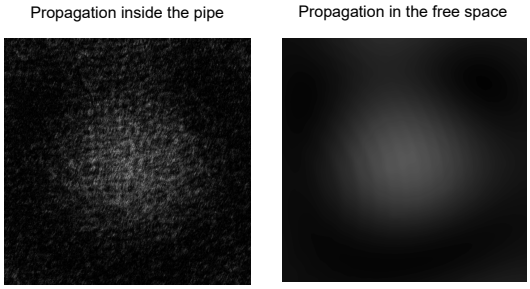

Figure 8: IC image comparison for SLB propagation over 140 m in a reflective vacuum pipe and free space.

A 2 m laboratory setup was used to test the influence of different pipe types and their positions with respect to the SLB axis. The noise created by the 50 mm diameter stainless steel pipe is depicted in Fig. 9

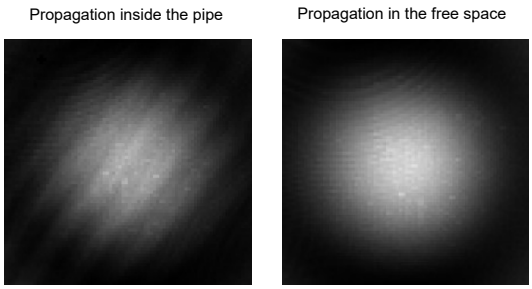

Figure 9: IC image comparison for SLB propagation over 2 m in a reflective pipe and free space.

The dependence of the result on the position of the pipe is illustrated in Fig. 10. The laboratory test compares images of the IC in free-space propagation for various transverse positions of the pipe. The propagation distance is 2 m and the diameter of each pipe is 50 mm. The transverse position

is defined such that a pipe position of 0 mm indicates that the pipe is centered around the beam axis. The pipe wall passes through the IC axis when the pipe wall is misaligned by 25 mm.

The pipe axis remains parallel to the beam axis throughout the experiment. A rough black plastic pipe and a reflective smooth stainless steel pipe were used for this experiment. The Structural Similarity Index Measure (SSIM) [19], shown on the y-axis, compares the image without the pipe to the image with the pipe at a certain position. If the images are the same, SSIM = 1. The index decreases as the amount of noise introduced by the pipe increases.

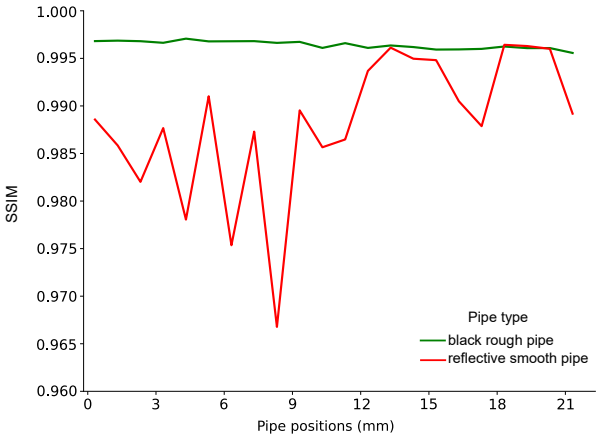

Figure 10: The comparison of noise provoked by reflective and absorbing pipes depending on the transverse position of the pipe.

An SLB is a result of the superposition of contributions from different areas of its wavefront and requires coherent light, such as that from a laser, to be generated. However, stray light in the vacuum pipe will interfere with the direct SLB pattern, complicating IC position detection and potentially causing issues in defining the straight reference line. To maximize performance, a non-reflective pipe is required for alignment applications over long distances.

CONCLUSION

An SLB offers a promising solution for long-distance alignment applications, particularly in large particle accelerators. Its pseudo-non-diffractive nature, characterized by a low-divergence Inner Core (IC) and prominent Outer Ring (OR), allows the creation of a straight reference line over distances previously unattainable with traditional Gaussian or Bessel beams. The SLB's performance, however, is influenced by various factors including generator parameters, changes in the refractive index of the traversed medium and interference from reflections. Addressing these factors through careful design and optimization, such as using vacuum systems to reduce atmospheric refraction and implementing non-reflective coatings, can enhance the precision and reliability of future SLB-based alignment systems.

Further research and experimental validation are ongoing to fully realize the potential of SLBs for practical applications. Investigating the symmetry breaking caused by an obstacle in both the near and far zones is crucial for maintaining the straightness of the reference line. Simulations should be supported by empirical tests to validate the predictions of symmetry breaking in various setups, and a comprehensive study of the effects of reflection on the IC detection accuracy.

REFERENCES

[1] M. Sulc and J.-C. Gayde, "An optical system for producing a Structured Beam." EP3564734, 2019.

[2] W. Niewiem, K. Polak, M. Dusek, D. Mergelkuhl, J.-C. Gayde, A. Wieser, and M. Sulc, "Variation of Structured Laser Beam pattern and optimization for an alignment reference line creation," *Optics Express*, vol. 31, p. 43307, 12 2023.

[3] D. M. Gale, "Visual alignment of mechanical structures using a Bessel beam datum: practical implementation," in *Optical Measurement Systems for Industrial Inspection VII*, vol. 8082, p. 80823D, International Society for Optics and Photonics, SPIE, 2011.

[4] R. E. Parks, "Aligning reflecting optics with Bessel beams," in *Optical System Alignment, Tolerancing, and Verification XIII*, vol. 11488, p. 114880J, International Society for Optics and Photonics, SPIE, 2020.

[5] R. E. Parks, "Practical considerations for using grating produced Bessel beams for alignment purposes," in *Proc.SPIE*, vol. 11816, p. 1181603, 8 2021.

[6] D. M. Witold Niewiem, Jean-Christophe Gayde, "Refraction effects on a Structured Laser Beam as a reference line for alignment," in *Euspen's 24th International Conference and Exhibition, Dublin, IE*, Euspen, 2024.

[7] R. J. Leao, C. R. Baldo, M. L. C. D. C. Reis, and J. L. A. Trabanco, "Engineering survey planning for the alignment of a particle accelerator: Part I. proposition of an assessment method," *Measurement Science and Technology*, vol. 29, 2 2018.

[8] R. E. Ruland, "Alignment considerations for the next linear collider," in *Proceedings of the IEEE Particle Accelerator Conference*, vol. 3, pp. 2009–2013, IEEE, 1995.

[9] V. Rude, H. M. Durand, J. Pfingstner, and V. Boria, "Micrometric propagation of error using overlapping stretched wires for the CLIC prealignment," in *IPAC2017, Copenhagen, Denmark*, European Spallation Source, 2017.

[10] W. B. Herrmannsfeldt, "SLAC alignment system," *Proceedings of the 1966 Linear Accelerator Conference, Los Alamos, New Mexico, USA*, 1966.

[11] D. Kämtner and J. Prenting, "Straight line reference system (SLRS) for the adjustment of the x-ray free-electron laser (XFEL) at DESY," in *9th International Workshop on Accelerator Alignment*, 2006.

[12] G. Stern, "Study and development of a laser based alignment system for the Compact Linear Collider," *ETH Library*, 2016.

[13] J.-C. Gayde, K.Polak, and M. Sulc, "Introduction to Structured Laser Beam for alignment and status of the R&D," *16th International Workshop on Accelerator Alignment*, vol. 19, 2022.

[14] M. Satoh and T. Suwada, "Design of collimated laser beam optics for the KEKb injector linac alignment system," in *Proceedings of Linear Accelerator Conference LINAC2010, Tsukuba, Japan*, 2010.

[15] K. Polak, J.-C. Gayde, and M. Sulc, "Structured Laser Beam for alignment and large-scale metrology," in *Euspen's 22nd International Conference and Exhibition, Geneva, Switzerland*, p. 301–304, 2022.

[16] L. Mayer, B. Jeong, T. Brendel, R. Furfaro, V. Reddy, and D. Kim, "Scattering properties of black pigments: implications for detecting faint sources near the moon using ground-based telescopes," in *Astronomical Optics: Design, Manufacture, and Test of Space and Ground Systems IV*, vol. 12677, p. 126770B, International Society for Optics and Photonics, SPIE, 2023.

[17] M. Asadnezhad, A. Eslamimajd, and H. Hajghassem, "Stray light analysis, baffle, and optical design of a high-resolution satellite camera," *Journal of Applied Remote Sensing*, vol. 12, no. 2, p. 026009, 2018.

[18] M. Dusek, E. Roikova, D. Mergelkuhl, J.-C. Gayde, K. Polak, and M. Sulc, "Analysis of centroiding algorithms for non-diffracting structured and hollow Structured Laser Beams," *Appl. Opt.*, vol. 63, pp. 263–274, Jan 2024.

[19] Z. Wang, A. Bovik, H. Sheikh, and E. Simoncelli, "Image quality assessment: from error visibility to structural similarity," *IEEE Transactions on Image Processing*, vol. 13, no. 4, pp. 600–612, 2004.